



Mg diffusion in Si on a thermodynamic basis

V. Saltas¹ · A. Chroneos^{2,3} · F. Vallianatos¹

Received: 7 February 2018 / Accepted: 27 April 2018 / Published online: 21 May 2018
© The Author(s) 2018

Abstract

In the present work, magnesium diffusion in silicon studied recently in the temperature range 600–1200 °C (Astrov et al. in *Phys Status Solidi A* 214:1700192, 2017; Shuman et al. in *Semiconductors* 51:5, 2017) is investigated on the basis of the $cB\Omega$ thermodynamic model, which connects point defect parameters with the macroscopic elastic and expansion properties. The calculated activation Gibbs free energy, activation enthalpy, activation entropy, activation volume and activation specific heat of Mg diffusion exhibit non-linear temperature dependence, due to the anharmonic behavior of the isothermal bulk modulus of Si. The calculated activation enthalpy of diffusion (1.67–2.12 eV) is in agreement with the reported experimental value (1.83 ± 0.02 eV) of Mg diffusion in Si, whereas the calculated activation volume (60% of the mean atomic volume) is compatible with the reported interstitial diffusion of Mg impurities.

1 Introduction

Silicon (Si) is the mainstream semiconductor material with applications in nanoelectronic, photovoltaics devices, and sensor applications [1–5]. Si has been intensively investigated over the past decades, however, recent experimental [time-of-flight secondary ions mass spectrometry (TOF-SIMS)] and theoretical advances [density functional theory (DFT)] have resulted in a better understanding of the defect process and diffusion mechanisms at an atomistic level [6–8]. This is important as the intrinsic point defects (i.e. vacancies, V and self-interstitials, I) effectively facilitate self- and dopant diffusion in Si and other group IV semiconductors such as germanium [6–8].

The defect processes of magnesium (Mg) in Si have been studied for numerous years [9–13]. From a technological viewpoint the interest is driven by the potential application of Mg-doped Si in photonic devices [14]. Mg in Si is

a divalent donor with a low solubility of Mg interstitials (Mg_i) of the order of 10^{15} cm^{-3} [15, 16]. Interestingly, it was determined by Sigmund that the concentration of Mg can be up to 10^{19} cm^{-3} at 1200 °C [17]. Recent experimental diffusion studies in dislocation free Mg-doped Si employed the p - n junction method and Hall measurements to indicate that mainly Mg_i migrate [12, 13].

In previous studies we employed thermodynamic approaches in conjunction with experimental techniques and/or DFT to gain an understanding of point defect properties in doped Si [18, 19]. These methods effectively connect the defect Gibbs free energy g^i ($i = f$ for defect formation, act for self-diffusion activation, or m for migration) with bulk properties in the crystalline solid [20–24]. The $cB\Omega$ model by Varotsos and Alexopoulos [22–26] (g^i is proportional to the isothermal bulk modulus B and the mean volume per atom Ω) is an efficient way to describe the defect processes in materials [20–26]. In particular, the $cB\Omega$ model has been employed to describe a range of systems (oxide fluorites, diamond, Si, AgI, Ge, ZnO, GaAs) for numerous applications (including for example electronic, nuclear, geophysical) [27–37].

In the present study, the recently reported experimental data [12, 13] on diffusion of Mg in Si in the temperature range, 873–1473 K are analyzed in the framework of the $cB\Omega$ model. Based on reported elastic and expansion properties of Si, we calculate the corresponding temperature dependence of various point defect thermodynamic parameters such as activation enthalpy, activation Gibbs free

✉ V. Saltas
vsaltas@chania.teicrete.gr

✉ A. Chroneos
alexander.chroneos@imperial.ac.uk

¹ School of Applied Sciences, Technological Educational Institute of Crete, Heraklion, Greece

² Department of Materials, Imperial College London, London SW7 2AZ, UK

³ Faculty of Engineering, Environment and Computing, Coventry University, Priory Street, Coventry CV1 5FB, UK

energy, activation entropy, activation volume and specific heat of activation. Our predictions are discussed with respect to reported experimental results.

2 Methodology

2.1 The $cB\Omega$ model

The $cB\Omega$ model has been developed on the substantiated thermodynamic basis [24] that the Gibbs free energy of activation (formation or migration) of a point defect is proportional to the isothermal bulk modulus B and the mean volume per atom Ω of the host material, i.e.

$$g^{act} = c^{act} B\Omega \quad (1)$$

here, c^{act} is a dimensionless constant that is temperature and pressure independent under certain experimental conditions [24]. In this regard, the diffusion coefficients D of a dopant in a monoatomic crystal, via a single mechanism, are given by the following modified Arrhenius equation

$$D(T) = fga_0^2 \nu e^{-c^{act} B\Omega/k_B T} \quad (2)$$

where the diffusion correlation factor f depends on the diffusion mechanism and the crystal structure, g is a geometric factor, a_0 is the lattice parameter, ν is the attempt frequency and k_B is Boltzmann's constant.

The temperature (or pressure) dependence of various point defect parameters of diffusion, for example the activation entropy s^{act} , activation enthalpy h^{act} , activation volume v^{act} and specific heat of activation c_p^{act} , according to Eq. (1), is exclusively a function of the elastic and expansion properties of the bulk material, through the following relations

$$s^{act} = - \left. \frac{\partial g^{act}}{\partial T} \right|_P = -c^{act} \Omega \left\{ \left. \frac{\partial B}{\partial T} \right|_P + \beta B \right\} \quad (3)$$

$$h^{act} = g^{act} + Ts^{act} = c^{act} \Omega \left\{ B - T \left(\beta B - \left. \frac{\partial B}{\partial T} \right|_P \right) \right\} \quad (4)$$

$$v^{act} = - \left. \frac{\partial g^{act}}{\partial P} \right|_T = c^{act} \Omega \left\{ \left. \frac{\partial B}{\partial P} \right|_T - 1 \right\} \quad (5)$$

and

$$c_p^{act} = \left. \frac{\partial h^{act}}{\partial T} \right|_P = -c^{act} \Omega T \left\{ \beta^2 B + 2\beta \left. \frac{\partial B}{\partial T} \right|_P + B \left. \frac{\partial \beta}{\partial T} \right|_P + \left. \frac{\partial^2 B}{\partial T^2} \right|_P \right\} \quad (6)$$

here, β denotes the volumetric coefficient of thermal expansion, $\beta = \Omega^{-1}(\partial\Omega/\partial T|_P)$ and is also temperature and pressure dependent. The activation volume is a useful point defect parameter, as it provides a fingerprint of the mechanism of the diffusion process.

In the previous Eqs. (1) and (3–6), the constant c^{act} can be determined by the mean value method which is applied in cases where experimental diffusion data is available on a broad range of temperatures [27, 31]. Specifically, by taking the decimal logarithm of both sides in Eq. (2), we obtain

$$\log D = \log (fga_0^2 \nu) - c^{act} (\log e) \frac{B\Omega}{k_B T} \quad (7)$$

According to Eq. (7), a linear relation between the values $\log D$ of the experimental diffusion coefficients and the calculated quantity $B\Omega/k_B T$ implies the validity of the $cB\Omega$ model for the case of a single diffusion mechanism, while c^{act} is derived directly from the slope of the linear fit.

2.2 Bulk properties of Si

Accurate measurements of the lattice parameter of high-purity crystalline Si in a wide temperature range (300–1500 K) has been reported by Okada and Tokumaru [38]. From their experimental results, they derived an empirical formula of the linear thermal expansion coefficient, as follows

$$a_l(T) = \left(3.725 \left(1 - e^{-5.88 \times 10^{-3}(T-124)} \right) + 5.548 \times 10^{-4} T \right) \times 10^{-6} \text{ K}^{-1} \quad (8)$$

Based on these findings, the mean atomic volume per atom Ω of the diamond cubic crystal lattice of Si and its linear thermal expansion coefficient a_l are depicted in Fig. 1a, b. A 2nd order polynomial, $\Omega (\times 10^{-30} \text{ m}^3) = 19.97 + 1.82 \times 10^{-4} T + 3.61 \times 10^{-8} T^2$ was sufficient to fit accurately ($R^2 = 0.999$) the experimental data of Ω in the entire temperature range.

The isothermal bulk modulus $B(T)$ of Si is derived from the relation [37, 39]

$$B(T) = \frac{B_s}{1 + \beta\gamma T} \quad (9)$$

where B_s stands for the adiabatic bulk modulus for which experimental data has been reported over the temperature range 293–1273 K [40], β is the volumetric coefficient of thermal expansion ($\beta = 3a_l$) and $\gamma (= 0.367)$ is the Grüneisen constant of Si [41]. The calculated isothermal bulk modulus of Si with respect to temperature is shown in Fig. 1c. In the medium temperature range (400–900 K) B varies almost linearly with temperature, while at higher temperatures ($T > 900$ K) a deviation from linearity is clearly observed. This deviation has been also reported for other solids at temperatures near their melting point [42]. Since the diffusion data of Mg in Si considered in the present study extends to higher temperatures (873–1473 K), a 2nd order polynomial $[B(\text{GPa}) = 79.2 + 2.44 \times 10^{-2} T - 1.73 \times 10^{-5} T^2, R^2 = 0.998]$ was used to fit the isothermal bulk modulus in

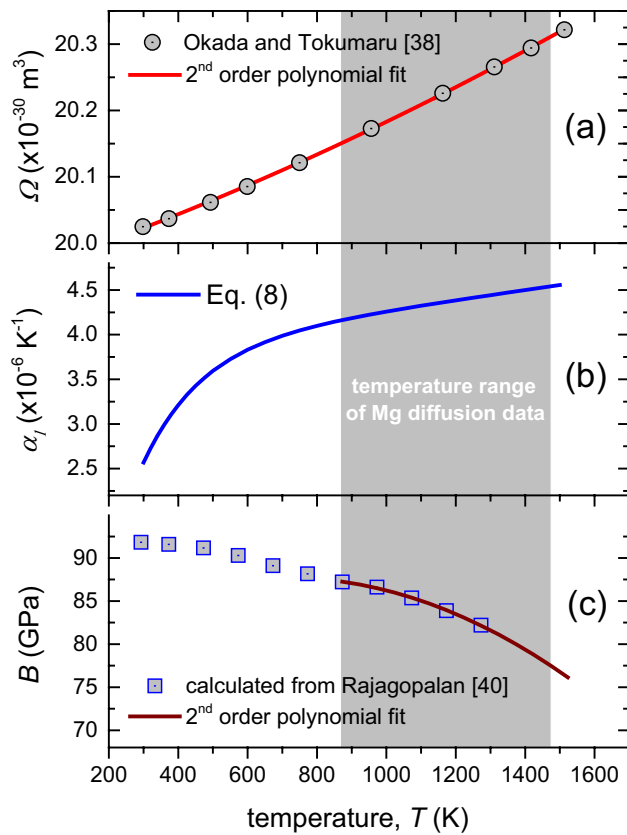


Fig. 1 Temperature dependence of Si bulk properties in the temperature range 300–1500 K. **a** The mean volume per atom Ω . **b** the linear thermal expansion coefficient α_l according to Eq. (8) and **c** the isothermal bulk modulus B , calculated from reported experimental data of the adiabatic bulk modulus [40], according to Eq. (9). A 2nd order polynomial fit was used to extrapolate data at temperatures of the reported experimental Mg diffusion data (873–1473 K)

the range 873–1273 K and extrapolate its values to higher temperatures, up to 1473 K. As a consequence, the temperature derivative of the isothermal bulk modulus $\partial B/\partial T|_P$ which is used in Eqs. (3), (4) and (6) follows a linear behavior.

Recently, the pressure derivative of isothermal bulk modulus of Si has been reported to be $(\partial B/\partial P)_T = 5.08$ at ambient pressure [43]. This value was used for the calculation of activation volumes using Eq. (5). Other reported values of $(\partial B/\partial P)_T$ derived from Murnaghan equation do not affect considerably the calculated activation volumes [18, 44]. These bulk properties of Si can also be used for the implementation of the $cB\Omega$ model in the study of any other dopant diffusion in crystalline Si [18].

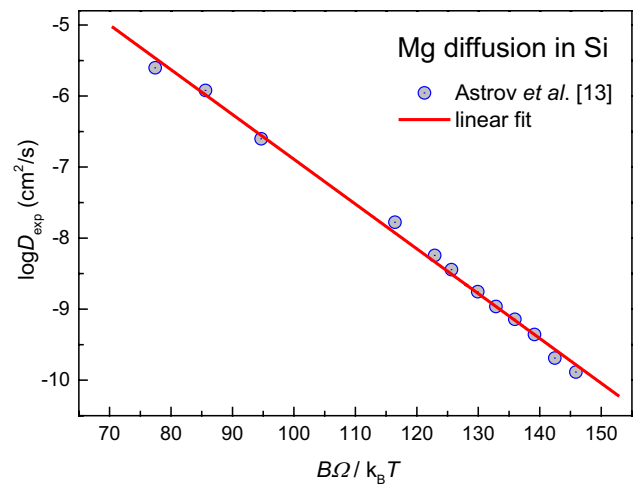


Fig. 2 The experimental diffusion coefficients of Mg in Si as a function of the dimensionless quantity, $B\Omega/k_B T$. The linear fit of the data ($R^2=0.996$) implies the validity of the $cB\Omega$ model, according to Eq. (7)

3 Results and discussion

Mg diffusion in dislocation-free Si has recently been investigated by Astrov et al. and by Shuman et al., in a broad temperature range (873–1473 K) [12, 13]. Astrov et al. [13] reported that the temperature dependence of Mg diffusion coefficients obeys to a single Arrhenius equation, as follows

$$D(T) = (5.3 \pm 1.0) \times \exp\left(-\frac{1.83 \pm 0.02 \text{ eV}}{k_B T}\right) \text{ cm}^2/\text{s} \quad (10)$$

To the best of our knowledge, no other experimental diffusion data of Mg in Si has been reported so far.

The reported experimental diffusion coefficients D_{exp} of Mg in Si with respect to the calculated dimensionless quantity $B\Omega/k_B T$ are shown in Fig. 2. It should be noted here that as Ω increases with T , at the same time isothermal bulk modulus B decreases (refer to Fig. 2a, c), and thus their product $B\Omega$ remains almost constant. Actually, $B\Omega$ determines the activation Gibbs free energy through Eq. (1) and exhibits a rather small variation with temperature, as shown afterwards. Consequently, $\log D_{\text{exp}}$ decreases linearly with the quantity $B\Omega/k_B T$. According to Eq. (6), the linear correlation of these two quantities ($R^2 = 0.996$) suggests the validity of the $cB\Omega$ model. From the slope of the linear fit, the value of the parameter c^{act} was calculated to be 0.1452 ± 0.0028 .

The experimental diffusion coefficients of Mg in Si and the corresponding calculated values (solid line) according to the $cB\Omega$ model are shown in the Arrhenius plot of Fig. 3. There is a good agreement between experimental and calculated values that allow proceeding further to the calculation of various point defect parameters. Specifically,

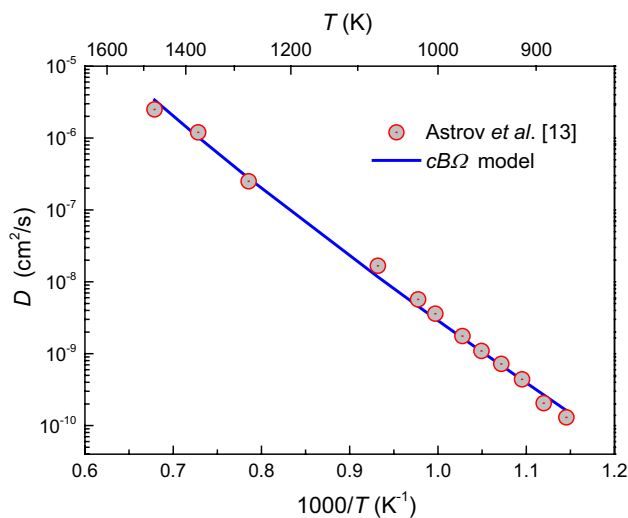


Fig. 3 Experimental diffusion coefficients of Mg in Si as a function of inverse temperature (Arrhenius plot). The solid line refers to the calculated values, according to the $cB\Omega$ model

activation Gibbs free energy (g^{act}), activation enthalpy (h^{act}), the energy term Ts^{act} , activation entropy (s^{act}) as well as the specific heat of activation have been plotted in Fig. 4 as a function of temperature, in the range 873–1473 K where the experimental diffusion data of Mg have been reported. A non-linear, monotonic temperature dependence is observed for the three energy terms, i.e. g^{act} , h^{act} and Ts^{act} (refer to Fig. 4a), while, with regard to activation enthalpy and specific heat of activation a linear increase is observed in both cases (refer to Fig. 4b). The ranges of the values of the aforementioned point defect parameters along with their calculated uncertainties are summarized in Table 1. Furthermore, the corresponding reported values of self-diffusion as well as of Ni and Cu fast diffusion in Si are also included in Table 1, for comparison. The experimental value of Mg activation enthalpy (1.83 eV) lies in our calculated range of values (1.67–2.12 eV).

The concept of temperature-dependent thermodynamic properties of point defects has been adopted by Kube et al., in the case of self-diffusion in Si over a broad temperature range (923–1661 K) [47]. In their study, they assumed a linear variation of activation enthalpy with temperature for vacancy defects to explain the non-linear Arrhenius behavior of self-diffusion coefficients. However, their assumption has been interpreted in the framework of the $cB\Omega$ model by Saltas et al. [37], where the non-linear anharmonic behavior of the bulk modulus of Si (refer to Fig. 1c) has inevitably resulted in the temperature dependence of activation enthalpy, according to Eq. (4). In this context, the temperature dependent bulk properties of Si influence all the other calculated point defect parameters (refer to Eqs. 1, 3, 5 and 6), which also exhibit temperature dependence, as in the

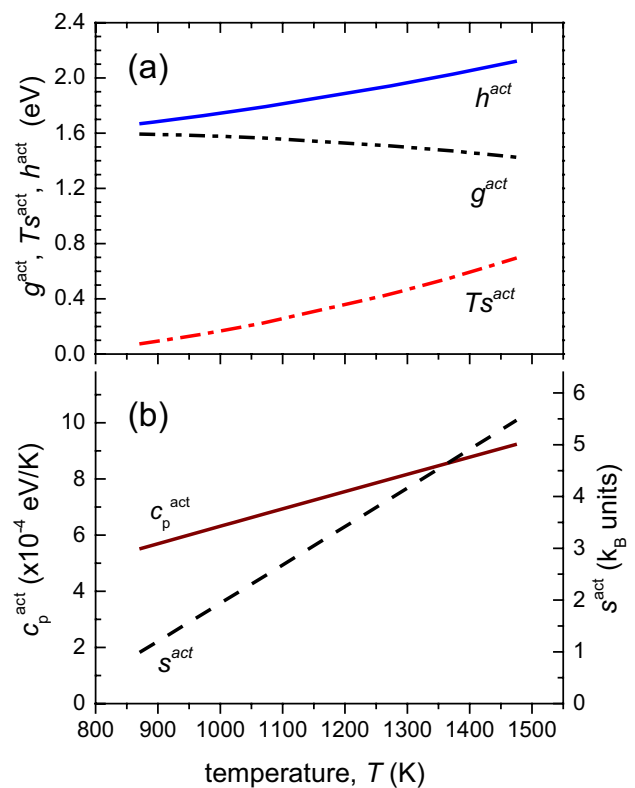


Fig. 4 Calculated point defect parameters of Mg diffusion in Si in the temperature range of the corresponding experimental diffusion data (873–1473 K). **a** Activation Gibbs free energy g^{act} , activation enthalpy h^{act} and the energy term Ts^{act} . **b** Activation entropy s^{act} and specific heat of activation c_p^{act}

present case or in previous study of Ni and Cu fast diffusion in Si [18]. On the contrary, in the case of tin diffusion in Ge [48], the linear behavior of bulk modulus of Ge in the temperature range 828–1203 K does not cause significant variation of the activation enthalpy and other calculated point defect parameters.

Finally, we have to mention that in all cases of self- or hetero-diffusion in Si (refer to Table 1), the temperature dependence of v^{act} is negligible due to the constant value of $(\partial B/\partial P)_T$ and the slow varying mean atomic volume Ω , according to Eq. (5). In the present case of Mg diffusion in Si, the calculated values of activation volume correspond to $\sim 60\%$ of the mean atomic volume at room temperature, Ω_0 (refer to Table 1). Shuman et al. reported that the Mg diffusion in Si occurs mainly via the interstitial mechanism [12]. If Mg is indeed diffused in interstitial sites, the corresponding activation volume of diffusion does not include any defect formation and thus it would be equal to the migration volume, $v_I^m = v^s - v^{eq}$, i.e. the volume difference between the equilibrium (v^{eq}) and the saddle-point position (v^s). If the diffusion mechanism would involve the formation of vacancies, we would expect higher values of activation volumes, as

Table 1 Calculated values of the parameter c^{act} , activation enthalpy (h_{calc}^{act}), activation entropy (s^{act}), activation Gibbs free energy (g^{act}) and activation volume (v^{act}), according to the $cB\Omega$ model, for diffu-

sion in Si. The corresponding reported values of Ni, Cu and self-diffusion in Si are also included for comparison

Element	Temp. (K)	c^{act}	h_{calc}^{act} (eV)	h_{exp}^{act} (eV)	s^{act} (k_B units)	g^{act} (eV)	c_p^{act} ($\times 10^{-4}$ eV/K)	v^{act} ($\times 10^{-29}$ m ³)
Mg	873–1473	0.1452 ± 0.0028	$(1.67-2.12) \pm 0.12$	1.83 ± 0.02 [13]	$(1.01-5.46) \pm 0.30$	$(1.59-1.43) \pm 0.10$	$(5.52-9.22) \pm 0.38$	$(1.19-1.20) \pm 0.14$ ($0.60 \Omega_0$)
Ni	938–1158	0.0126 ± 0.0009	$(0.146-0.159) \pm 0.031$	0.15 ± 0.04 [45]	$(0.11-0.25) \pm 0.07$	$(0.134-0.138) \pm 0.034$	–	0.071 ± 0.015 ($0.036 \Omega_0$)
Cu	265–1173	0.0149 ± 0.0004	$(0.168-0.189) \pm 0.039$	0.18 ± 0.01 [46]	$(-0.12$ to $0.31) \pm 0.09$	$(0.171-0.158) \pm 0.041$	–	0.084 ± 0.016 ($0.042 \Omega_0$)
Si [37]	923–1661	0.311 ± 0.004	$(3.56-4.92) \pm 0.11$	$3.66-4.71$ [47]	$(2.0-14.6) \pm 0.3$	$(2.83-3.41) \pm 0.09$	–	$(2.56-2.58) \pm 0.17$ ($1.29 \Omega_0$)

in the case of vacancy-mediated self-diffusion in Si where, $v^{act} = 1.29 \Omega_0$ (refer to Table 1) [37].

4 Conclusions

In the present work, the recently reported experimental data of Mg diffusion in Si is investigated in the framework of a thermodynamic model which allows the calculation of point defect parameters from the macroscopic bulk properties of the host material. Based on accurately reported experimental elastic and expansion properties of Si, the Gibbs free energy, enthalpy, entropy, volume and specific heat of activation were calculated as a function of temperature in the range, 873–1473 K. All these quantities are temperature dependent due to the anharmonic behavior of the isothermal bulk modulus of Si. The calculated activation enthalpy is in agreement with the recently reported experimental value and the corresponding activation volume suggests the interstitial diffusion mechanism. The present study can serve as a paradigm to related work on the defect processes of semiconductors and oxides [49–52].

Open Access This article is distributed under the terms of the Creative Commons Attribution 4.0 International License (<http://creativecommons.org/licenses/by/4.0/>), which permits unrestricted use, distribution, and reproduction in any medium, provided you give appropriate credit to the original author(s) and the source, provide a link to the Creative Commons license, and indicate if changes were made.

References

1. S. Takeuchi, Y. Shimura, O. Nakatsuka, S. Zaima, M. Ogawa, A. Sakai, Appl. Phys. Lett. **92**, 231916 (2008)
2. A. Chroneos, C.A. Londos, E.N. Sgourou, J. Appl. Phys. **110**, 093507 (2011)
3. E. Kamiyama, K. Sueoka, J. Vanhellefont, J. Appl. Phys. **111**, 083507 (2012)
4. C. Gao, X. Ma, J. Zhao, D. Yang, J. Appl. Phys. **113**, 093511 (2013)
5. P. Chen, X. Yu, X. Liu, X. Chen, Y. Wu, D. Yang, Appl. Phys. Lett. **102**, 082107 (2013)
6. R. Kube, H. Bracht, A. Chroneos, M. Posselt, B. Schmidt, J. Appl. Phys. **106**, 063534 (2009)
7. R. Kube, H. Bracht, J.L. Hansen, A.N. Larsen, E.E. Haller, S. Paul, W. Lerch, J. Appl. Phys. **107**, 073520 (2010)
8. A. Chroneos, H. Bracht, Appl. Phys. Rev. **1**, 011301 (2014)
9. H. Sigmund, D. Weiss, in *Ion Implantation: Equipment and Techniques*, vol. 11 ed. by H. Ryssel, H. Glawischnig eds. Springer Series in Electrophysics, (Springer, Berlin, 1983), p. 473
10. V.M. Arutyunyan, A.P. Akhoyan, Z.N. Adamyan, R.S. Barsegyan, Tech. Phys. **71**, 67 (2001)
11. F. Legrain, O.I. Malyi, S. Manzhos, Solid State Ionics **253**, 157 (2013)
12. V.B. Shuman, A.A. Lavrent'ev, Yu.A. Astrov, A.N. Lodygin, L.M. Portsel, Semiconductors **51**, 5 (2017)
13. Yu.A. Astrov, V.B. Shuman, L.M. Portsel, A.N. Lodygin, S.G. Pavlov, N.V. Abrosimov, V.N. Shastin, H.-W. Hübers, Phys. Status Solidi A **214**, 1700192 (2017)
14. V.N. Shastin, V.V. Tsyplenkov, R.K. Zhukavin, K. Kovaleskii, Y. Astrov, H.-W. Hübers, S.G. Pavlov, in *Proceedings of the XVIII Symposium on Nanophysics and Nanoelectronics*. Nizhny Novgorod, Russia, p. 678, (2014)
15. R.F. Franks, J.B. Robertson, Solid State Commun. **5**, 479 (1967)
16. L.T. Ho, A.K. Ramdas, Phys. Rev. B **5**, 462 (1972)
17. H. Sigmund, J. Electrochem. Soc. **129**, 2809 (1982)
18. V. Saltas, A. Chroneos, F. Vallianatos, J. Appl. Phys. **123**, 161527 (2018)
19. V. Saltas, D. Horlait, E.N. Sgourou, F. Vallianatos, A. Chroneos, Appl. Phys. Rev. **4**, 041301 (2017)
20. P. Varotsos, K. Alexopoulos, Phys. Rev. B **15**, 4111 (1977)
21. P. Varotsos, K. Alexopoulos, Phys. Rev. B **15**, 2348 (1977)
22. P. Varotsos, W. Ludwig, K. Alexopoulos, Phys. Rev. B **18**, 2683 (1978)
23. P. Varotsos, K. Alexopoulos, Phys. Rev. B **30**, 7305 (1984)
24. P. Varotsos, K. Alexopoulos, *Thermodynamics of Point Defects and Their Relation with the Bulk Properties* (North-Holland, Amsterdam, 1986)
25. P. Varotsos, N. Sarlis, M. Lazaridou, Phys. Rev. B **59**, 24 (1999)
26. P. Varotsos, J. Appl. Phys. **101**, 123503 (2007)
27. B.H. Zhang, X.P. Wu, Appl. Phys. Lett. **100**, 051901 (2012)
28. F. Vallianatos, K. Eftaxias, Phys. Earth Planet. Inter. **71**, 141 (1992)
29. F. Vallianatos, V. Saltas, Phys. Chem. Miner. **41**, 181 (2014)
30. E.S. Skordas, Solid State Ionics **261**, 26 (2014)
31. V. Saltas, F. Vallianatos, Mater. Chem. Phys. **163**, 507 (2015)
32. A. Chroneos, R.V. Vovk, Solid State Ionics **274**, 1 (2015)
33. M.W.D. Cooper, R.W. Grimes, M.E. Fitzpatrick, A. Chroneos, Solid State Ionics **282**, 26 (2015)

34. A. Chroneos, *Appl. Phys. Rev.* **3**, 041304 (2016)
35. V. Saltas, A. Chroneos, F. Vallianatos, *RSC Adv.* **6**, 53324 (2016)
36. V. Saltas, A. Chroneos, F. Vallianatos, *Sci. Rep.* **7**, 1374 (2017)
37. V. Saltas, A. Chroneos, F. Vallianatos, *Mater. Chem. Phys.* **181**, 204 (2016)
38. Y. Okada, Y. Tokumaru, *J. Appl. Phys.* **56**, 314 (1984)
39. O.L. Anderson, *J. Phys. Chem. Solids* **27**, 547 (1966)
40. S. Rajagopalan, *IL Nuovo Cimento* **51**, 222 (1979)
41. D.S. Kim, H.L. Smith, J.L. Niedziela, C.W. Li, D.L. Abernathy, B. Fultz, *Phys. Rev. B* **91**, 014307 (2015)
42. J. Garai, A. Laugier, *J. Appl. Phys.* **101**, 023514 (2007)
43. F. Decremps, L. Belliard, M. Gauthier, B. Perrin, *Phys. Rev. B* **82**, 104119 (2010)
44. J.Z. Hu, I.L. Spain, *Solid State Commun.* **51**, 263 (1984)
45. J. Lindroos, D.P. Fenning, D.J. Backlund, E. Verlage, A. Gorgulla, S.K. Estreicher, H. Savin, T. Buonassisi, *J. Appl. Phys.* **113**, 204906 (2013)
46. A.A. Istratov, C. Flink, H. Hieslmair, E.R. Weber, T. Heiser, *Phys. Rev. Lett.* **81**, 1243 (1998)
47. R. Kube, H. Bracht, E. Hüger, H. Schmidt, J.L. Hansen, A.N. Larsen, J.W. Ager III, E.E. Haller, T. Geue, J. Stahn, *Phys. Rev. B* **88**, 085206 (2013)
48. Y. Panagiotatos, V. Saltas, A. Chroneos, F. Vallianatos, *J. Mater. Sci.: Mater. Electron.* **28**, 9936 (2017)
49. E.N. Sgourou, D. Timerkaeva, C.A. Londos, D. Aliprantis, A. Chroneos, D. Caliste, P. Pochet, *J. Appl. Phys.* **113**, 113506 (2013)
50. N.V. Sarlis, E.S. Skordas, *Solid State Ionics* **290**, 121 (2016)
51. B.H. Zhang, J.S. Xu, *AIP Adv.* **6**, 115112 (2016)
52. N.P. Kobelev, V.A. Khonik, *J. Exp. Theor. Phys.* **126**, 340 (2018)